Organic LETTERS

Letter

pubs.acs.org/OrgLett

Commiphoranes A–D, Carbon Skeletal Terpenoids from *Resina Commiphora*

Lu Dong,[†,‡,∥] Li-Zhi Cheng,[†,‡,∥] Yong-Ming Yan,[†] Shu-Mei Wang,[‡] and Yong-Xian Cheng*[,†]

[†]State Key Laboratory of Phytochemistry and Plant Resources in West China Kunming Institute of Botany, Chinese Academy of Sciences, Kunming 650201, PR China

[‡]Guangdong Pharmaceutical University, Guangzhou 510006, PR China

Supporting Information

ABSTRACT: Commiphoranes A–D (**1**–**4**), four novel aromatic terpenoids with unprecedented carbon skeletons, were isolated from *Resina Commiphora*. Their structures were identified by spectroscopic and crystallographic methods. Compounds **1** and **2** are dinorditerpenoids characteristic of a 6/6/6/6 ring system. In contrast, compounds **3** and **4** are sesquiterpenoids possessing a 5/6/7 backbone. Biological evaluation reveals that **3** could significantly attenuate overproduction of fibronectin, collagen I, and α-SMA in TGF-β1-induced rat renal proximal tubular cells.

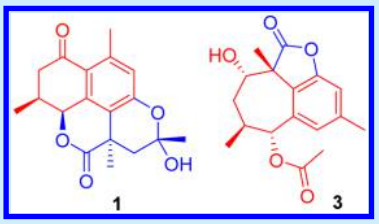

Plant resins are defined primarily as lipophilic mixtures of volatile and nonvolatile terpenoids and/or phenolic compounds.[1] Many plants could produce resins, notable examples of plant resins are amber, copal from trees of *Protium copal*, dammar gum from trees of the family Dipterocarpaceae, Dragon's blood from dragon trees (*Dracaena* species), frankincense from *Boswellia sacra*, and so on. Plants secrete resins usually for their protective benefits such as defending against herbivores, insects, and pathogens.[2] However, plant resins have been commercially used since ancient times. They are important sources for the production of incense and perfume. Among the most plant resins, it is notable that several resins are medicinally used, exemplified by Dragon's blood, catechu, benzoin, and gamboge. We have become interested in medicinal plant resins in recent years, and previous study revealed GQ5 from *Toxicodendron vernicifluum* to be a specific p-Smad3 inhibitor,[3] implying its potential in renal fibrosis. In the course of our continuing investigations on plant resins, *Resina Commiphora* generally known as myrrh was conducted. *Resina Commiphora* is the resinous exudates of the genus *Commiphora* (Burseraceae) such as *C. myrrha*, which has been used for a long time in the traditional medicines of India, Greece, Rome, and Babylon.[4] Its use medicinally in PR China began from A.D. 600 during Tang Dynasty. Nowadays, it is commonly prescribed together with frankincense (a resin from *Boswellia*) to treat a wide range of disorders including pain, swelling, trauma, arthritis, ulcer, and sore.[5,6] Previous investigation of the genus *Commiphora* revealed more than 300 secondary metabolites with diverse activities.[7] In the present study, four novel terpenoids with new carbon skeletons, commiphoranes A–D (**1**–**4**), were isolated and structurally identified. Their biological activities against renal fibrosis were evaluated in TGF-β1-induced rat renal proximal tubular cells.

Commiphorane A (**1**),[8] obtained as a colorless needle (in methanol), was found to have a molecular formula $C_{18}H_{20}O_5$ by analysis of its HRESIMS, ^{13}C NMR, and DEPT spectra, indicating nine degrees of unsaturation. The ^1H NMR spectrum of **1** exhibits four methyl groups and one olefinic/aromatic proton. The ^{13}C NMR and DEPT spectra (Table S1) reveal 18 carbon signals classified into four methyl, two methylene, three methine (one olefinic, two aliphatic with one oxygenated), and nine quaternary carbons (one ketone, one carbonyl, five olefinic including one oxygenated, one hemiacetal, and one aliphatic). The structure construction of **1** was mainly aided by interpretation of its 2D NMR data. The $^1H-^1H$ COSY spectrum discloses interactions of H-3/H-4/H-5 and H-4/H_3-14. These spin systems, in consideration of HMBC correlations of H-3, H-4/C-2 (δ_C 195.6), imply the presence of an isoprenyl residue (part I) (Figure 1). Further HMBC correlations of H_3-15/C-1 (δ_C 121.1), C-10 (δ_C 141.5), C-9 (δ_C 120.0), in conjunction with olefinic nature of C-1, suggest the presence of another isoprenyl moiety (part II), which is thereafter known to embrace C-6 (δ_C

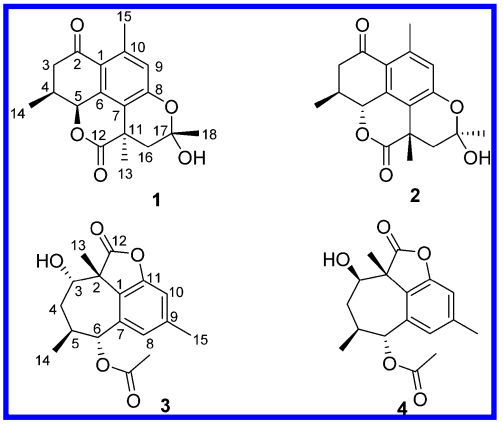

Figure 1. Structures of **1**–**4**.

Received: December 8, 2016
Published: December 28, 2016

DOI: 10.1021/acs.orglett.6b03661
Org. Lett. 2017, 19, 286–289

136.8) in this fragment. Additional HMBC correlations of H_3-13/C-11, C-12 (δ_C 173.5), C-7 (δ_C 117.5), in consideration of the chemical shift of C-7 (sp^2), indicate that there exists the third isoprenyl fragment (part III). In fact, the observed pivotal HMBC correlations of H-9/C-7, C-8 and relatively weak cross peak of H-9/C-11, not only indicate the formation of a $\Delta^{7,8}$ double bond, but also reveal that parts II and III are connected via C-8. With these data in hand, **1** is apparently a terpenoidal derivative. In the HMBC spectrum, correlations of H-16/C-17, C-18 and H_3-18/C-16, C-17 are observed, indicating the presence of fragment C-16-C-17-C-18 (part IV), which is confirmed to connect with part III via C-11 evident from HMBC correlations of H-16/C-7, C-11,C-12, C-13. Thus far, parts II–IV were assembled. As far as construction of parts I and II is concerned, it is rather challengeable due to the absence of available HMBC data. The chemical shift of C-2 discloses the presence of a conjungated ketone, in accordance with the observation of a UV absorbance at 277 nm. Besides, a pivotal HMBC cross peak between H-5/C-7, in consideration of olefinic and quaternary nature of C-6, suggests the only possibility of C-5-C-6-C-7 and C-2-C-1. In this way, a pentasubstituted benzene ring is naturally assembled. This conclusion is also in line with the biogenetic standpoint of terpenoidal derivatives. In addition to ring A (Figure 2), a benzene ring (B), a ketone, and a carbonyl

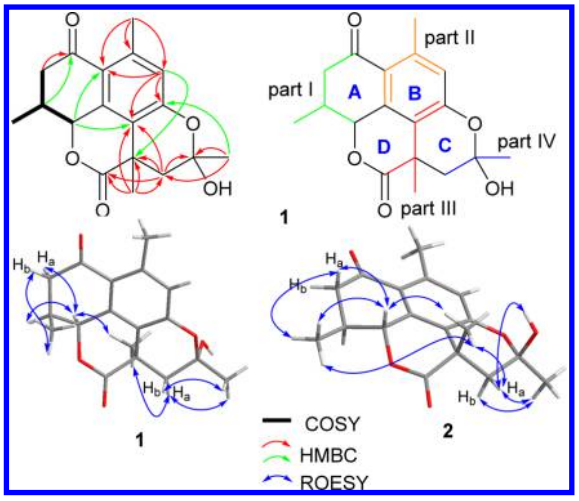

Figure 2. Key COSY and HMBC correlations of **1** (green in **1** recorded in $CDCl_3$) and ROESY correlations of **1** and **2**. Green, orange, red, and blue colors in **1** represent four independent isoprenyl moieties or parts I–IV.

(C-12), accounting for seven degrees of unsaturation, the remaining two degrees of unsaturation require the presence of two rings. The chemical shifts of C-8 (δ_C 154.4) and C-17 (δ_C 98.6) and a weak HMBC correlation of H_3-18/C-8 suggest hemiacetal nature of C-17 and the formation of ring C. Despite the absence of HMBC correlation between H-5/C-12 ($^3J_{H,C}$), the carbon resonances at C-5 and C-7 is indicative of a lactone (ring D), in consistence with the relatively downfield shift of C-5 (δ_C 76.3) arising from ring tension. Taken together, the planar structure of **1** was identified.

The relative configuration of **1** was assigned by a ROESY experiment, which shows correlations of H-5/Ha-3, H_3-14/Hb-3, and H-5/H_3-13, revealing the orientations of H_3-14, H-5, and H_3-13. Meanwhile, H-5 correlating with H_3-13 exceptionally confirms the presence of ring D. For the orientation of H_3-18, ROESY correlations of H_3-13/Ha-16 and H_3-18/Ha-16, Hb-16 are observable. In a molecular model study, these restrictions appear possible only when ring C adopts a half chair conformation and H_3-18 is at an equatorial position. This conclusion is further confirmed by X-ray diffraction analysis using CuKa radiation (Figure 3),[9] which also allows to assign the absolute configuration of **1** as 4*S*,5*S*,11*R*,17*S*.

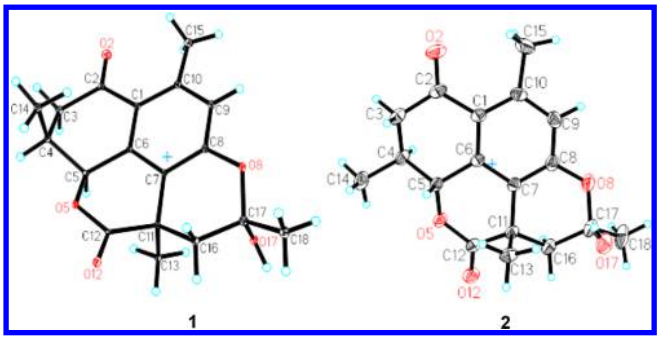

Figure 3. X-ray structures of **1** and **2** showing absolute configurations.

It is notable that part IV in **1** is actually an isoprenyl moiety losing two carbons at C-17. This alternation, to our knowledge, makes **1** a novel dinorditerpenoid with an unprecedented carbon skeleton. In addition, the formation of rings A–D via two O atom bridges makes **1** a rare 6/6/6/6 polycyclic system.

Commiphorane B (**2**)[10] possesses the same molecular formula as that of **1**. A detailed interpretation of 1D and 2D NMR data of **2** reveals that compounds **1** and **2** have the same planar architecture differing in their configurations at stereogenic centers. ROESY correlations (Figure 2) of H-5/H_3-13, H_3-14, Ha-3, H_3-14/Ha-3, H_3-13, and H_3-13, 17-OH/Ha-16 are observable, indicating the relative configuration of **2**. Compound **2** was obtained as a colorless needle (in methanol), subsequent X-ray diffraction analysis using CuKα radiation assigned the absolute configuration of **2** as 4*S*,5*R*,11*S*,17*R* (Figure 3).[11] Apparently, compound **2** is a C-4 epimer of the enantiomer of **1**.

Commiphorane C (**3**)[12] has a molecular formula $C_{17}H_{20}O_5$ as determined on the basis of its HRESIMS, ^{13}C NMR, and DEPT spectra, suggesting eight degrees of unsaturation. The ^1H NMR spectrum of **3** shows four methyl groups and two olefinic/aromatic protons (Table S2). The ^{13}C NMR and DEPT spectra indicate 17 carbon resonances ascribe to four methyl, one methylene, five methine (two olefinic, three aliphatic with two oxygenated), and seven quaternary carbons (two carbonyls, four olefinic with one oxygenated, one aliphatic). The structure elucidation of **3** was performed using a combination of 2D NMR experiments. The ^1H–^1H COSY spectrum gives correlations of H-3/H-4/H-5/H-6 and H-5/H_3-14. HMBC correlations of H_3-13/C-1, C-2, C-3, C-12 (δ_C 179.7), H-3 (δ_H 4.24)/C-13, H-4/C-2, and H-6/C-1, C-7 indicate that the two isoprenyl residues construct ring A (Figure 4). Further, HMBC correlations of H_3-15/C-8, C-9, C-10, H-8/C-10, C-15, and H-10/C-8, C-11, C-15 imply the presence of an additional isoprenyl moiety. This fragment is connected with ring A via C-7-C-8 supported by the observed HMBC correlations of H-6/C-7, C-8 and H-8/C-1 (Figure 4). Olefinic nature of C-1 and C-11 suggests that a double bond is built between these two carbons, in accordance with a biogenetic point of view. In this way, a benzene ring (B) is formed, which makes **3** an aromatic sesquiterpenoid. Similar compounds with an aromatic ring in the structure were actually found in natural origins. Apart from rings A and B, two carbonyls, the remaining one degree of unsaturation requires the presence

DOI: 10.1021/acs.orglett.6b03661
Org. Lett. 2017, 19, 286–289

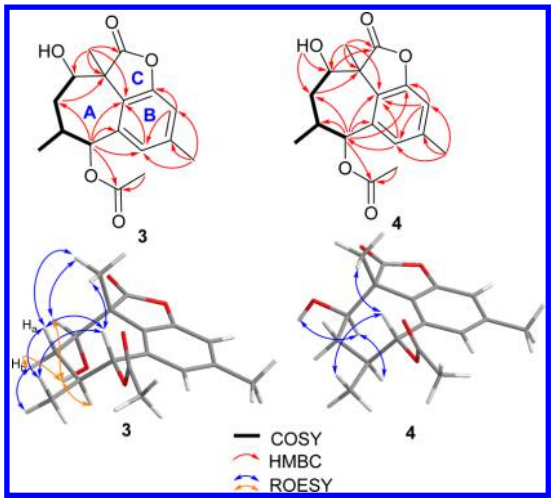

Figure 4. Key COSY, HMBC and ROESY correlations of **3** (orange in **3** recorded in DMSO-d_6) and **4**.

of a ring. The chemical shift of C-12 and absence of tailing behavior on TLC plate indicates the possible formation of a lactone. However, there have three possibilities for the position of such a lactone. HMBC correlations of C$\underline{H_3}$CO, H-6/CH$_3\underline{C}$O exclude the possibility of a six-membered lactone. ROESY correlations of OH/H-3, Hb-4, H-5 indicate a free OH group attached to C-3 (δ_C 71.1). The chemical shift of C-11 (δ_C 153.5) and the negative color reaction by spraying $FeCl_3$-reagent indicates construction of a five-membered lactone (ring C). Thus far, the planar structure of **3** was identified. The formation of rings A−C in **3** makes it a 5/6/7 ring system and an unprecedented carbon skeleton sesquiterpenoid.

The relative configuration of **3** was clarified by using ROESY data. In the ROESY spectrum, correlations of H_3-13/H-6, H-3, Ha-4, and H-6/Ha-4, H_3-14 are observed (Figure 4), indicating the relative configurations at ring A. As a result, the structure of **3** was finally determined.

Commiphorane D (**4**)[13] was found to have the same planar structure with that of **3** by extensive analysis of its 2D NMR spectra. The only difference between **4** and **3** is the relative configuration at C-3 gained support from ROESY correlations of H_3-13/H-6, H-6/H_3-14, and H-3/H-5 (Figure 4). Of note, HMBC correlations of H-10/C-1, 3-OH/C-3, C-4, and a weak correlation of H-6/C-11 are observed in **4** rather than in **3**, which add further evidence for structures **3** and **4**. In addition, it is apparent that compound **4** is a C-3 epimer of **3**.

As is shown in Scheme 1, a plausible biosynthetic pathway for terpenoids **1**−**4** starts from farnesyl pyrophosphate (FPP) whose enzymatic cyclization affords the intermediate A. Oxidation and esterification of A produces B. Dehydration of B results in C. Carbocation at C-8 of the intermediate C formed by hydrogen ion reacts with isopentenyl pyrophosphate (IPP) under prenyltransferase to yield D. Subsequent electrophilic substitution and cyclization of D generates E. Oxidation and retro-aldol reaction of E produces the intermediate F. Ultimately, commiphoranes A and B (**1** and **2**) were created by nucleophilic addition−elimination reaction. Starting from FPP, cyclization of FPP affords G. Reduction of G under nicotinamide adenine dinucleotide phosphate (NADPH) followed by multistep oxidation, esterification, and acetylization produce commiphoranes C and D (**3** and **4**).

Organ fibrosis can lead to progressive dysfunction of liver, lung, kidney, heart, and eventually death of patients. Therefore,

Scheme 1. Plausible Pathway for the Biogenesis of 1−4

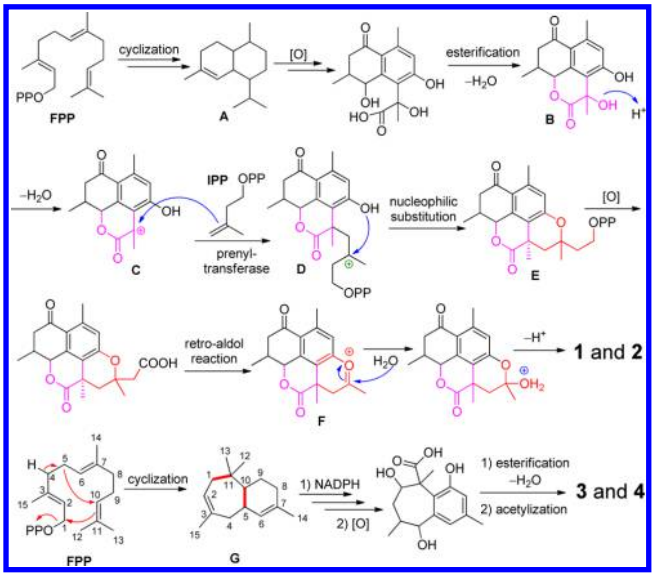

search for antifibrotic therapy has received attention in recent years. According to the philosophy of traditional Chinese medicine, herbs with function of promoting blood circulation are usually used for intervention of fibrosis;[14,15] therefore, compounds from *Resina Commiphora*, which possess blood circulation, blood promoting, and blood stasis removing effects, are decided to check their antifibrotic activities. Regardless of different etiologies, organ fibrosis shares a common pathogenetic process: excessive activation of the key profibrotic cytokine TGF-β accompanied by extracellular matrix overexpression. With this, antifobrotic activities of **1**−**4** were carried out in TGF-β1-induced rat renal proximal tubular cells (Figure 5). The results

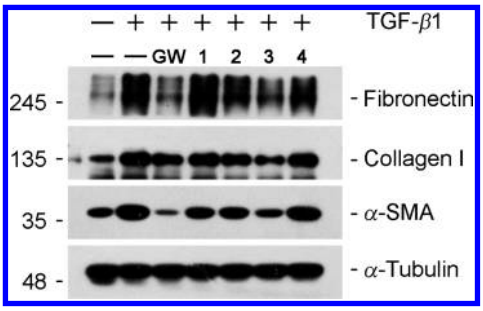

Figure 5. Compounds **1**−**4** inhibit fibrogenic action of TGF-β1 in rat renal proximal tubular cells. NRK-52E cells were incubated with TGF-β1 (5 ng/mL) for 48 h in the absence or presence of compounds **1**−**4** (20 μM). Cell lysates after treatments as indicated were immunoblotted with antibodies against fibronecitn, collagen I, α-SMA, and α-tubulin. GW: GW788388, Medchemexpree (MCE), HY-10326.

show that **1**−**3** could significantly reduce overproduction of collagen I and that α-SMA with **3** is the most active. Although compounds **2** and **3** both attenuate fibronectin overexpression, **3** is much stronger than **2**. Despite slight structural difference between **3** and **4**, whereas **4** is inactive toward the indicated proteins. Considering that TGF-β1/Smads pathway is central mediators of fibrosis,[16] the mechanism of **3** was further examined (Figure 6). It was found that **3** does not affect phosphorylation of Smad2/3, indicating that the effects of **3** are embodied through non-Smad pathway.

DOI: 10.1021/acs.orglett.6b03661
Org. Lett. 2017, 19, 286−289

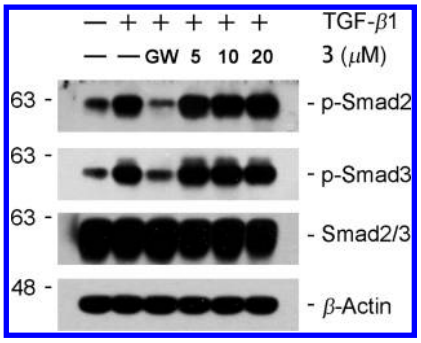

Figure 6. Compound **3** does not block TGF-β1-mediated Smad2 and Smad3 phosphorylation. NRK-52E cells were treated with TGF-β1 (5 ng/mL) for 3 h in the absence or presence of different concentrations (5 to 20 μM) of **3** as indicated. Cell lysates after various treatments were immunoblotted with antibodies against phosphorylated Smad2, phosphorylated Smad3, total Smad2/3, and β-actin. GW: GW788388, Medchemexpree (MCE), HY-10326.

■ ASSOCIATED CONTENT

Supporting Information

The Supporting Information is available free of charge on the ACS Publications website at DOI: 10.1021/acs.orglett.6b03661.

One- and two-dimensional , and MS spectra, detailed isolation procedures, crystallographic data, and bioassay methods (PDF)

■ AUTHOR INFORMATION

Corresponding Author

*Phone/fax: +86-871-65223048. E-mail: yxcheng@mail.kib.ac.cn.

ORCID

Yong-Xian Cheng: 0000-0002-1343-0806

Author Contributions

‖These authors contributed equally to this work.

Notes

The authors declare no competing financial interest.

■ ACKNOWLEDGMENTS

This study was supported by National Science Fund for Distinguished Young Scholars (81525026).

■ REFERENCES

(1) Langenheim, J. H. *Taxon* **2003**, *52*, 647−658.
(2) Becerra, J. X. *Ecology* **1994**, *75*, 1991−1996.
(3) Ai, J.; Nie, J.; He, J. B.; Guo, Q.; Li, M.; Lei, Y.; Liu, Y. H.; Zhou, Z. M.; Zhu, F. X.; Liang, M.; Cheng, Y. X.; Hou, F. F. *J. Am. Soc. Nephrol.* **2015**, *26*, 1827−1838.
(4) Shen, T.; Yuan, H. Q.; Wan, W. Z.; Wang, X. L.; Ji, M.; Lou, H. X. *J. Nat. Prod.* **2008**, *71*, 81−86.
(5) Al-Harbi, M. M.; Qureshi, S.; Raza, M.; Ahmed, M. M.; Afzal, M.; Shah, A. H. *J. Ethnopharmacol.* **1997**, *55*, 141−150.
(6) Abdul-Ghani, R. A.; Loutfy, N.; Hassan, A. *Parasitol. Int.* **2009**, *58*, 210−214.
(7) Shen, T.; Li, G. H.; Wang, X. N.; Lou, H. X. *J. Ethnopharmacol.* **2012**, *142*, 319−330.
(8) Commiphorane A (**1**): colorless needles; $[\alpha]_D^{22}$ −67.5 (*c* 0.23, MeOH); UV (MeOH) λ_{max} (log ε) 277 (4.12), 230 (4.18) 213 (4.13) nm; CD (MeOH) $\Delta\varepsilon$211 +16.81, $\Delta\varepsilon$236 −20.32, $\Delta\varepsilon$280 −3.05; ESIMS (positive) *m*/*z* 339 $[M + Na]^+$; HRESIMS *m*/*z* 355.0943 $[M + K]^+$ (calcd for $C_{18}H_{20}KO_5$ 355.0942); ^{1}H and ^{13}C NMR data, see Table S1.
(9) Crystallographic data of commiphorane A (**1**) have been deposited at the Cambridge Crystallographic Data Centre (deposition no. CCDC 1497060). Copies of the data can be obtained free of charge via www.ccdc.cam.an.uk/conts/retrieving.html.
(10) Commiphorane B (**2**): colorless needles; $[\alpha]_D^{22}$ +69.8 (*c* 0.15, MeOH); UV (MeOH) λ_{max} (log ε) 276 (4.25), 230 (4.32), 213 (4.25), 196 (4.10) nm; CD (MeOH) $\Delta\varepsilon$210 −34.61, $\Delta\varepsilon$236 +34.90, $\Delta\varepsilon$281 +4.43; ESIMS (positive) *m*/*z* 339 $[M + Na]^+$; HRESIMS *m*/*z* 355.0945 $[M + K]^+$ (calcd for $C_{18}H_{20}KO_5$ 355.0942); ^{1}H and ^{13}C NMR data, see Table S1.
(11) Crystallographic data of commiphorane B (**2**) have been deposited at the Cambridge Crystallographic Data Centre (deposition no. CCDC 1497061). Copies of the data can be obtained free of charge via www.ccdc.cam.an.uk/conts/retrieving.html.
(12) Commiphorane C (**3**): colorless gum; $[\alpha]_D^{25}$ +48.7 (*c* 0.05, MeOH); UV (MeOH) λ_{max} (log ε) 273 (3.37), 204 (4.55) nm; ESIMS (positive) *m*/*z* 327 $[M + Na]^+$; HRESIMS *m*/*z* 327.1202 $[M + Na]^+$ (calcd for $C_{17}H_{20}NaO_5$ 327.1208); ^{1}H and ^{13}C NMR data, see Table S2.
(13) Commiphorane D (**4**): colorless gum; $[\alpha]_D^{22}$ +29.1 (*c* 0.10, MeOH); UV (MeOH) λ_{max} (log ε) 373 (3.06), 205 (4.31) nm; ESIMS (positive) *m*/*z* 327 $[M + Na]^+$; HRESIMS *m*/*z* 327.1207 $[M + Na]^+$ (calcd for $C_{17}H_{20}NaO_5$ 327.1208); ^{1}H and ^{13}C NMR data, see Table S2.
(14) Liu, M.; Chen, M. H.; Zhao, Q. L. *Int. J. Chin. Tradit. Med.* **2014**, *36*, 1146−1148.
(15) Liu, X. P.; Yang, L. L.; Fu, P.; Tang, K. L.; Cao, Z. W. *Shengwu Wuli Xuebao* **2012**, *28*, 971−982.
(16) Zhang, Y. E. *Cell Res.* **2009**, *19*, 128−139.

DOI: 10.1021/acs.orglett.6b03661
Org. Lett. 2017, 19, 286−289